Subtle variations in polymer chemistry modulate substrate stiffness and fibronectin activity

Nayrim Brizuela Guerra,†[a] Cristina González-García,†[a] Virginia Llopis,[a] Jose Carlos Rodríguez-Hernández,[a] David Moratal,[a] Patricia Rico*[ab] and Manuel Salmerón-Sánchez*[abc]

Received 8th March 2010, Accepted 3rd June 2010
DOI: 10.1039/c0sm00074d

A family of polymer substrates which consists of a vinyl backbone chain with the side groups $-COO(CH_2)_xCH_3$, with $x = 0$, 1, 3, 5 was prepared. Substrates with decreasing stiffness, characterised by the elastic modulus at 37 °C, and similar chemical groups were obtained. Firstly, we have investigated whether these minute variations in polymer chemistry lead to differences in fibronectin (FN) adsorption: the same FN density was obtained on every substrate (450 ng cm^{-2}) but the supramolecular organisation of the protein at the material interface, as obtained with AFM, was different for $x = 0$ and the other surfaces ($x = 1$, 3, 5). Consequently, this allows one to use a set of substrates ($x = 1$, 3, 5) to investigate the effect of substrate stiffness on cell behavior as the unique physical parameter, *i.e.* after ruling out any influence of the length of the side group on protein conformation. Moreover, the importance of investigating the intermediate layer of proteins at the cell-material interface is stressed: the effect of $x = 0$ and $x = 1$ on cell behavior cannot be ascribed to the different stiffness of the substrate anymore, since the biological activity of the protein on the material surface was also different. Afterwards, initial cellular interaction was investigated using MC3T3-E1 osteoblasts-like cells and focusing on actin cytoskeleton development, focal adhesion formation and the ability of cells to reorganize the adsorbed FN layer on the different substrates. Image analysis was used to quantify the frequency distribution of the focal plaques, which revealed broader distributions on the stiffer substrates, with formation of larger focal plaques revealing that cells exert higher forces on stiffer substrates.

Introduction

It is now well known that cells interact with synthetic materials making use of an intermediate layer of matrix proteins previously adsorbed on the materials surface, coming from either the physiological fluids *in vivo* or culture medium *in vitro*, such as fibronectin (FN), vitronectin (VN) and fibrinogen (FG); representing the so-called soluble matrix proteins in the biological fluids.[1–3] Protein adsorption on material surfaces is a process driven by both the intensity of the energetic interactions—between the molecular groups of the substrate's surface and of the protein (*i.e.*, hydrogen bonding, electrostatic and van der Waals interactions)—and entropic changes as a consequence of the unfolding of the protein as bound water is released from the surface.[4,5] The activity of a protein on a synthetic surface, *i.e.* the concentration, distribution, and motility of the adsorbed protein layer on a surface, plays a fundamental role in the bio-functionality of a synthetic material and are clue factors to understand the biological response of a substrate.[6]

Cells recognize adsorbed matrix proteins *via* the integrin family of trans-membrane receptors that link the ECM to the actin cytoskeleton.[7] Integrins cluster after interacting with ECM proteins and may develop focal adhesions, which are discrete supramolecular complexes that contain structural proteins such as vinculin, talin, α-actinin, and signalling molecules, including FAK, Src and paxilin that actually anchor the cells to the surface and trigger the subsequent cellular response.[8] Thus, the initial cell-material interaction is a complex multi-step process consisting of early events, such as adsorption of proteins, followed by cell adhesion and spreading, and late events, related to cell growth, differentiation, matrix deposition and cell functioning. To measure and to quantify some of these parameters is the classical approach to characterising the cellular biocompatibility of materials.[9]

Even if the cell material interaction is not a direct one, but it is mediated by ECM proteins adsorbed on the substrate; it is said that cells response to three different kinds of surface properties: chemical, topographical and mechanical.[10] Mechanical properties of the substrate play an important role in cell response regardless of surface chemistry and topography but it is not completely understood yet. When cells are cultured on classic (rigid) polystyrene dishes, they develop micron-sized focal adhesions connected by actin fibers. However, these structures are gradually lost as cells are cultured on softer substrates, as prepared for example by changing the crosslinking density of gels[11–13] and, more recently, through polyelectrolyte multilayers.[13] Cell spreading and motility are higher on stiff substrates than on soft ones, which favours cell-cell interaction compared to

[a]*Center for Biomaterials and Tissue Engineering, Universidad Politécnica de Valencia, 46022 Valencia, Spain. E-mail: masalsan@fis.upv.es; parico@upvnet.upv.es; Fax: +34 963877276; Tel: +34 963877275*
[b]*CIBER de Bioingeniería, Biomateriales y Nanomedicina (CIBER-BBN), Valencia, Spain*
[c]*Regenerative Medicine Unit, Centro de Investigación Príncipe Felipe, Autopista del Saler 16, 46013 Valencia, Spain*
† These two authors contributed equally to this work.

the cell-material one and leads to more organised cell aggregates.[14] Cell proliferation increases on stiff surfaces and, in the case of a rigidity gradient on the substrate, cells migrate to stiffer regions.[15,16] This kind of cell behaviour has been found for different cells types (fibroblasts, muscular VSMC cells, chondrocytes and neurons) independently of the protein coating of the substrate (fibronectin, collagen, *etc*). It is thought that cells are able to react to substrate rigidity by means of a real tactile exploration, by exerting contractile forces and interpreting the substrate deformation.[12–22]

The relationship between the mechanical properties of the matrix and the activity of cells must lead to the maintenance of a functional mechanical state. The effect of substrate stiffness on the dynamic behaviour of surface associated matrix proteins is generally missing, *i.e.* is protein conformation somehow determined by substrate stiffness? Moreover, the preparation of substrates with controlled rigidity leads, most of the time, to small variations in substrate chemistry, *e.g.* by changing the crosslinking ratio in a polyacrylamide gel.[23] This work investigates the role of fibronectin adsorption on a family of polymers whose stiffness can be modulated by minute variations in material chemistry, *i.e.* just by sequentially adding methyl groups in the side group of a vinyl chain. FN was adsorbed on the different substrates and its supramolecular organisation followed by AFM. FN adsorption takes place in an equivalent way (in terms of the protein surface density and conformation) only for some substrates, which allows one to investigate the effect of substrate stiffness on cell behavior independently of surface chemistry, *i.e.* after assessing that subtle differences in polymer chemistry does not alter either the amount of adsorbed FN nor its conformation. Afterwards, cell adhesion on the different fibronectin-coated substrates was investigated and the frequency distribution of focal areas was quantified by image analysis.

Results

Material properties

The substrates investigated in this work consist of a vinyl backbone chain with the side groups $-COO(CH_2)_xCH_3$, where $x = 0$, 1, 3 and 5 (Fig. 1a). Fig. 1b shows the elastic moduli as measured in the tension mode at 37 °C. The stiffness of the substrate decreases monotonically as the number of methyl groups in the side chain, without modifying any other functionality of the system. Additionally the water contact angle increases 10° from PMA to the rest of the substrates, which display approximately the same wettability (Fig. 1c). The topography of the surfaces was examined by AFM prior to protein adsorption. Similar roughness parameters were obtained regardless of the polymer composition (arithmetic average of the height deviations from the center plane, Ra = 20 nm and standard deviation of the height values, Rms = 25 nm). We also scanned the surface of the materials after immersion in PBS (*i.e.* without FN) and no significant modification in roughness was found. The system x = 1, 3 and 5 is appropriate to investigate the influence of the stiffness of the substrate on the cell-protein-material interaction, after assessing the same pattern for FN adsorption.

Protein adsorption

The amount of FN adsorbed on the different surfaces was quantified by image analysis of the western blot bands. Calibration curves were built with known amounts of FN charged in

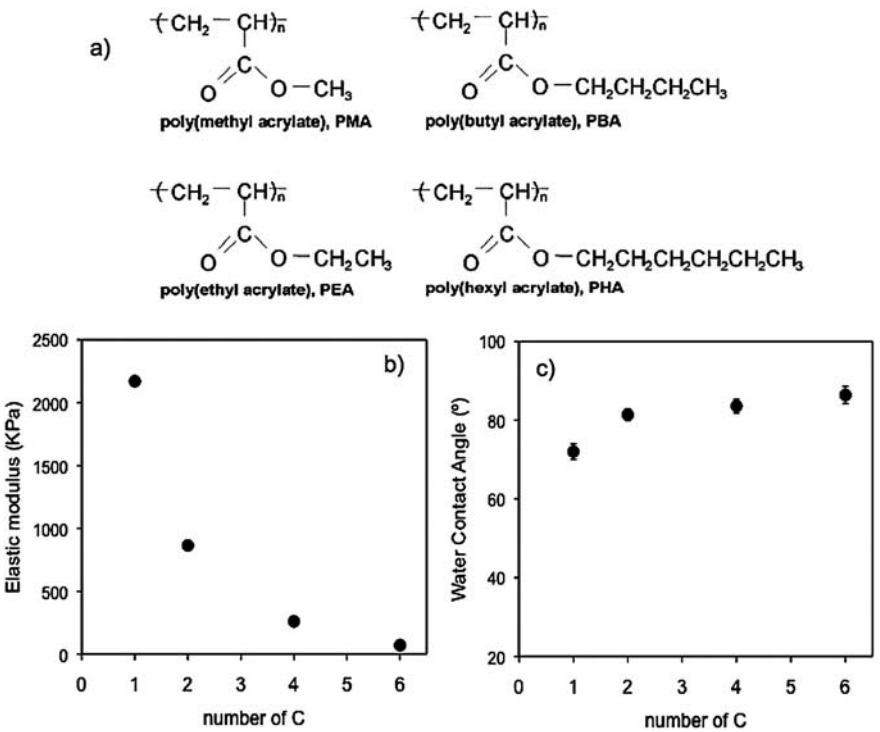

Fig. 1 The properties of the material substrates. (a) Chemical structure of the different substrates with increasing length of the side group: methyl (PMA), ethyl (PEA), butyl (PBA) and hexyl (PHA). (b) Substrate elastic modulus as a function of the length of the side group (number of C): PMA (1), PEA (2), PBA (4) and PHA (6), as obtained at 37 °C. (c) Water contact angles of the different substrates as a function of the length of the side group (number of C). The standard deviation of five independent measurements is included, when it is not visible it is lower than the size of the symbol.

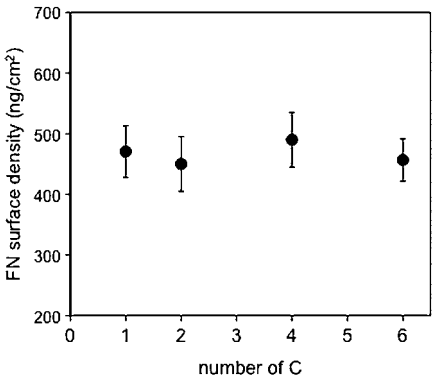

Fig. 2 The fibronectin surface density as a function of the length of the side group (number of C): PMA (1), PEA (2), PBA(4) and PHA (6). FN was adsorbed for 2 h from a solution of concentration 20 μg ml^{-1}.

the gel, *i.e.* different concentrations of the protein solution.[24] The calibration curve has been employed to quantify the amount of protein adsorbed on the different substrates. Each experiment included two calibration points so that the position of the whole calibration curve could be checked each time. Fig. 2 shows the results of the experiment on the different polymer substrates after adsorption from a FN solution of concentration 20 μg ml^{-1}. There is no significant difference among the amount of adsorbed FN on each substrate, which remains constant with a surface density of approximately 450 ng cm^{-2}.

Fig. 3 shows the AFM images of the adsorbed FN on the different substrates from protein solutions of different concentrations (as indicated in the figure) for 10 min. FN organisation and distribution on the surface depends, for each substrate, on

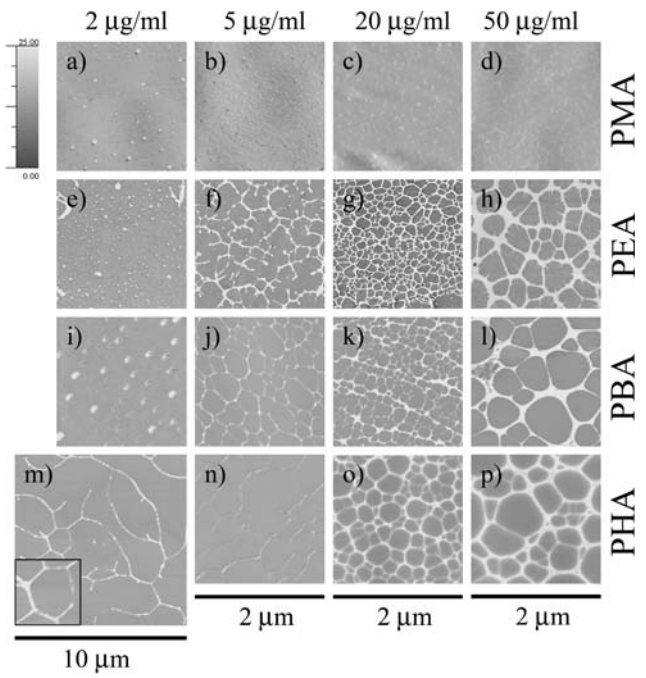

Fig. 3 The fibronectin distribution on the different substrates as observed by the phase magnitude in AFM. The protein was adsorbed for 10 min from different solutions of concentration 2 μg ml^{-1}, 5 μg ml^{-1}, 20 μg ml^{-1}, and 50 μg ml^{-1}.

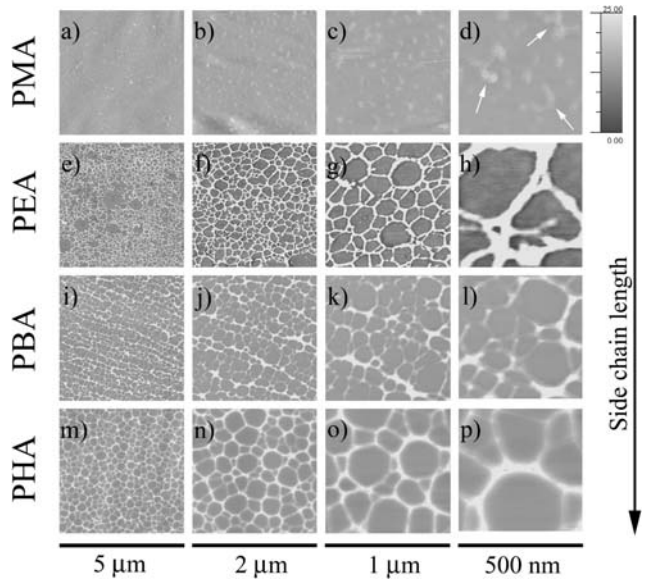

Fig. 4 The fibronectin distribution on the different substrates as observed by the phase magnitude in AFM at different magnifications. The protein was adsorbed for 10 min from a solution of concentration 20 μg ml^{-1}. The arrows in (d) show individual FN molecules.

the concentration of the initial protein solution from which the protein is adsorbed. The lowest concentration (2 μg ml^{-1}) results in isolated globular FN molecules homogeneously distributed on the material for PMA, PEA and PBA. However, the formation of long fibrillar FN structures is already observed on PHA after adsorption at this lowest concentration of the FN solution. For a concentration of 5 μg ml^{-1} (Fig. 3) globular protein molecules are still observed on PMA, but with higher density. However, the formation of an incipient network is already observed on PEA and a well interconnected one is observed on PBA and PHA. Protein adsorption from a solution of concentration 20 μg ml^{-1} gives rise to the formation of FN networks on PEA, PBA and PHA but not on PMA. Further increase of the concentration of the protein solution (50 μg ml^{-1}) gives rise to denser FN networks on PEA, PBA and PHA but only non-connected molecules remain on PMA.

Fig. 4 shows protein conformation and distribution at different magnifications (from 5 μm to 500 nm window) after adsorption on the different substrates from a 20 μg ml^{-1} protein solution, which is the concentration typically employed when coating a substrate with the protein for cell culture purposes.[29,30] Upon adsorption, FN organization into networks takes place on PEA, PBA and PHA but not on PMA. Only dispersed FN molecules are observed on the PMA substrate as the arrows in Fig. 4 point out.

Cell adhesion

FN activity on the different surfaces was addressed by evaluating the initial adhesion, after 3h, of MC3T3 osteoblast-like cells on the different FN-coated substrates and the control glass from a protein solution of concentration 20 μg ml^{-1}. Fig. 5 shows the overall morphology of cells *via* staining for actin (left column).

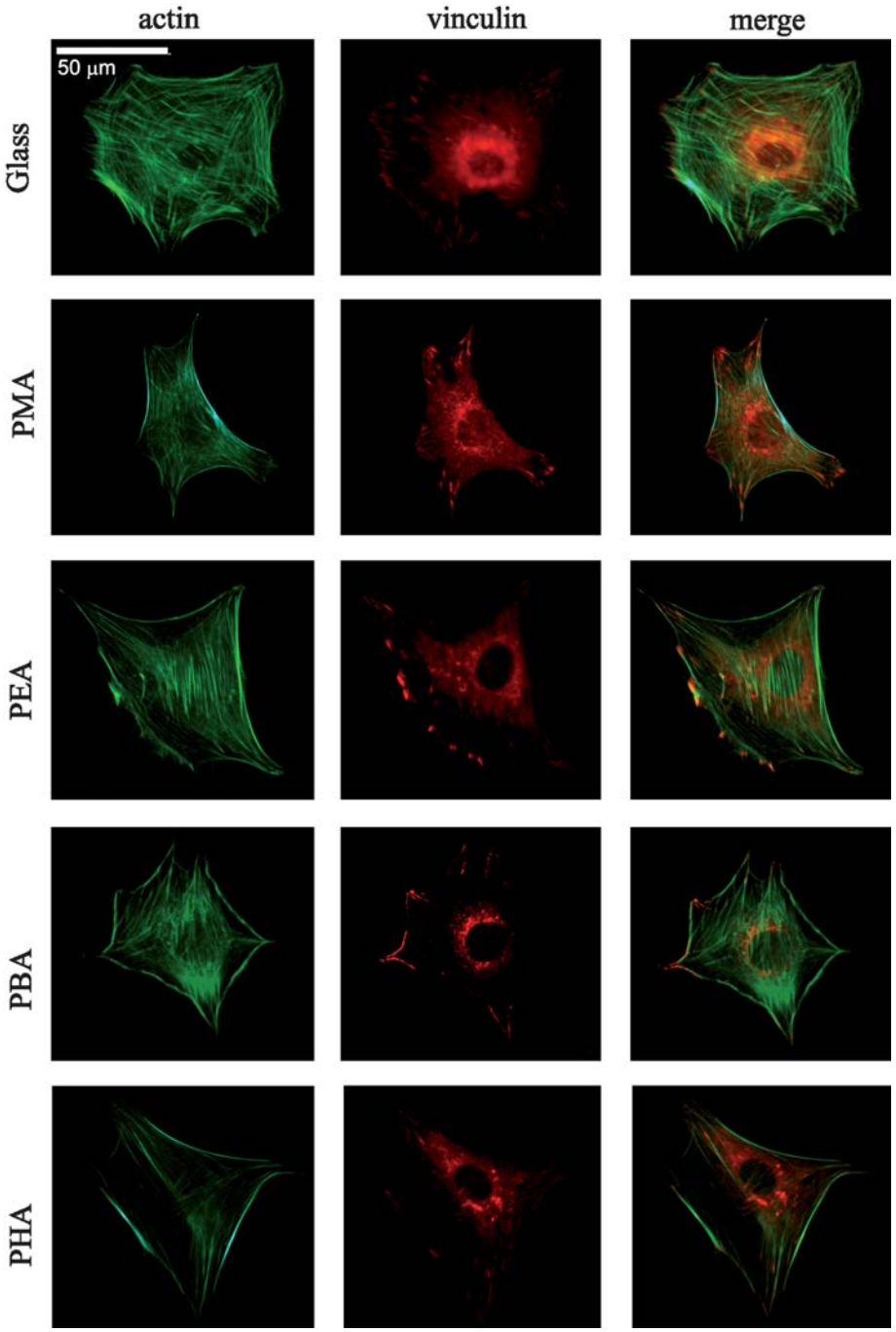

Fig. 5 MC3T3 osteoblast-like cells after 3 h on FN coated surfaces. The first column shows the F-actin cytoskeleton, the second column the focal adhesion plaques (vinculin). The third column is the superposition of the other two.

Cells presented prominent actin fibers inserting into well-developed focal adhesion complexes, as depicted in the central column for vinculin, especially for PMA and PEA. However, smaller focal contacts are observed on PBA and PHA. Moreover, the actin cytoskeleton is not completely developed on these substrates and only initial peripheral actin is shown. The area of the focal plaques was quantified by image analysis for representative cells on the different substrates and its frequency distribution is shown in Fig. 6. Small focal plaques are preferentially formed on PMA. Moreover, PEA shows the broader distribution of focal adhesion sites, which shrinks for PBA and PHA, as the stiffness of the substrate decreases.

Fig. 7 shows the cellular reorganisation of adsorbed FN after 3h of culture for the different substrates and the control glass. It is observed that cells are able to reorganise FN on the control glass as the dark area nearby the cell shows. Reorganisation also occurs actively on PMA, but only some movements of the adsorbed FN layer takes place on PEA, with smaller dark areas in the pericellular zone and mostly coincident with focal adhesion plaques. Moreover, reorganization is almost absent on PBA and

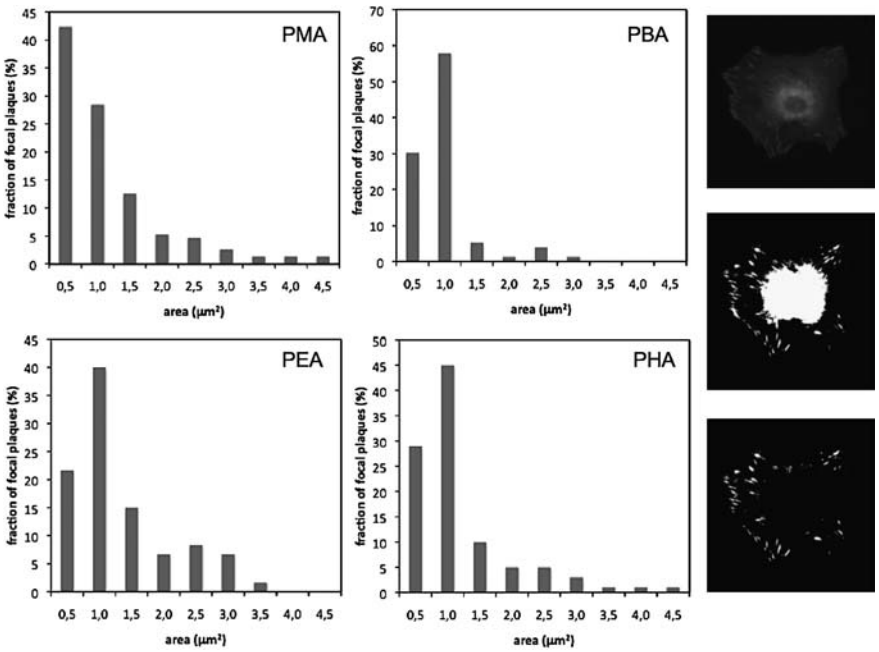

Fig. 6 The size distribution of focal adhesion plaques on the different substrates as quantified by image analysis. The picture shows the sequential process described in the text to delimitate focal adhesion plaques from the original image.

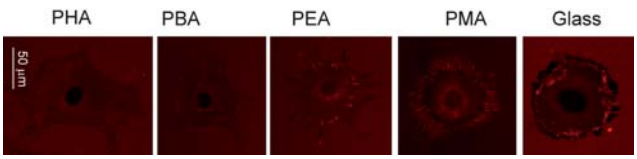

Fig. 7 The cellular reorganization of adsorbed FN on the different surfaces and control glass after 3h.

PHA on which the cell periphery is hardly distinguishable from the underlying FN layer on the substrate (Fig. 7).

Discussion

Matrix stiffness is known to determine overall cell fate: morphology, migration, differentiation, proliferation and apoptosis.[16,17,31] To understand the role of matrix stiffness on cell behaviour, extensive use has been made of substrates whose mechanical properties are varied by chemical modifications of the system. However, it is likely that the effects observed were partly a consequence of changes in surface chemistry, which is known to be an important factor that modulates the cell-material interaction.[32,33] We made use in this work of MC3T3-E1 preosteoblastic cells; when these cells were cultured on polyacrylamide substrates with different mechanical properties - achieved by changing the fraction of the crosslinker – proliferation and osteogenic differentiation were maximized on rigid substrates;[34] nevertheless, when the same cell line was cultured on alginate gels of similar mechanical moduli, they were found to differentiate better on the softer substrates.[35] Needless to say that these opposite results -with the same cell line and substrates of similar stiffness- must be a consequence of the different chemistries underlying the substrates used. Moreover, it points out the fact that surface chemistry cannot be underestimated when obtaining conclusions for cell response to the stiffness of the substrate.

Substrate chemistry influences the cell-material interaction by modulating the activity of the intermediate layer of proteins between the material substrates and the living cells: the amount of adsorbed protein and its conformation, which modulate integrin binding, focal adhesion composition and signalling.[36,37] The family of polymers used in this work allows one to prepare substrates of increasing stiffness (Fig. 1b) with minimum variation in polymer chemistry: a vinyl backbone with the side groups $–COO(CH_2)_xCH_3$, with $x = 0,1,3,5$. Only the stiffer substrate displays lower wettability (water contact angle (WCA) is approximately 10° lower) but the rest of them show no difference in WCA (Fig. 1c).

More importantly, however, is that protein adsorption on this family of substrates occurs in such a way that allows one to focus on the effects of substrate stiffness on cell behavior, even if there are subtle variations in the underlying chemistry. On the one hand, as approximately the same amount of FN is adsorbed on the substrates (Fig. 2), the measured FN surface density ($\approx$ 450 ng cm^{-2}) does not depend on the slightly different chemistries, which supports the intuitive idea that the amount of protein adsorbed does not depend on the stiffness of the substrate. On the other hand though, the distribution and conformation of the adsorbed FN, which determines its biological activity, shows some variations among substrates. PEA is a well studied polymer which is known to trigger FN organisation upon adsorption, leading to a so-called substrate induced fibronectin fibrillogenesis in absence of cells.[24,38,39] The dynamics of the assembly process for the FN network on PEA was followed by AFM, and the resulting supramolecular network has shown to be biologically active, driving cell adhesion, focal adhesion formation and matrix deposition.[38,39] Fig. 3 shows that to include either two or four additional methyl groups on the side chain of the polymer,

to obtain PBA and PHA, does also lead to the organisation of FN into networks on the substrate but with different dynamics. FN adsorption from solutions of increasing composition leads to the formation of a well-developed protein network at lower concentrations of the solution, as the number of methyl groups in the side chain of the polymer increases. That is to say, well-interconnected FN fibrils are found on PEA after adsorption from 20 μg ml^{-1} solution, on PBA after adsorption from 5 μg ml^{-1} solution and on PHA after adsorption from 2 μg ml^{-1} solution. Nevertheless, similar supramolecular organisation of the FN protein is found on PEA, PBA and PHA after adsorption from a solution of concentration 20 μg ml^{-1} (the one used to investigate the cell-material interaction) irrespective of the minute differences in material chemistry and, consequently, independently of the stiffness of the substrates. That major differences in FN adsorption take place mainly from solutions of low concentrations on substrates with similar chemistries has been previously reported.[40] There, two polymer substrates with very similar compositions, poly(DTD diglutarate) and poly-(DTD diglycolate), which differ in one single substitution of a methylene group by an oxygen atom in the polymer repeat unit were investigated. Treatment of the polymer surfaces with a FN solution of concentration 1 μg ml^{-1} lead to a pronounced decrease in FN activity on poly(DTD diglycolate) surfaces relative to poly(DTD diglutarate) ones, despite identical adsorbed levels of FN. However, no difference was found after adsorption from solutions of concentration 20 μg ml^{-1} on overall FN organization and conformation.[40]

The initial cellular interaction on this family of polymers allows one to investigate two different phenomena at the cell-material interface. Firstly, PMA and PEA with the same amount of adsorbed FN but in very different conformations were compared (Fig. 2 and 4). The difference between these two polymers must be sought in the ability of cells to rearrange the adsorbed protein layer after initial adhesion. Focal adhesion formation and actin development takes place in a similar way on FN-coated PMA and PEA but cells are able to reorganise FN on PMA and not on PEA (Fig. 7). On the other hand, by comparing results on PEA, PBA and PHA one must ascribe the different cell behavior to the decreasing stiffness of the substrate, since FN distribution and conformation does not vary among these substrates (Fig. 4). Focal adhesions play an essential role in cellular mechanosensing, including mechanochemical signal conversion and integrin clustering and strengthening of integrin-cytoskeleton linkages.[20,41] The total force transmitted by focal adhesions has been suggested to be proportional to their area.[42] Fig. 6 shows the distribution of focal adhesion sizes, as quantified from image analysis of representative cells on the different substrates. Once again, two independent conclusions can be extracted. The comparison between PMA and PEA, with different stiffness but also very different conformation of the adsorbed FN, shows a monotonically decreasing frequency distribution for cells on PMA, with most of the adhesion plaques (75%) below 1 μm^2; however, a more extended histogram is found on PEA with 40% of the focal plaques larger than 1 μm^2 and 25% above 2.5 μm^2. As the stiffness of the substrate decreases, the distribution of focal adhesions is narrower: more than 90 and 80% of the plaques are below 1 μm^2 for PBA and PHA respectively. This fact suggests that small focal adhesions are found on PMA with the appropriate size to transmit forces and remodel the adsorbed FN. The situation is different on PEA, and even being of lower stiffness than PMA, the very different biological activity of FN on these substrates (Fig. 4) leads to higher transmission of forces between the cell and the substrate, leading to the formation of larger focal plaques. That is to say, this is a good example of two very similar surface chemistries (PMA and PEA) on which as stiffness decreases the size of the focal plaques increases, but this effect must be ascribed to the very different activity of fibronectin upon adsorption on these substrates rather than the different mechanical properties of the substrate.

As the stiffness of the substrate diminishes, for the same FN organisation at the cell-material interface (PEA, PBA and PHA), the size of the focal adhesion plaques diminishes (Fig. 6) which must be a consequence of the lower magnitude of transmitted forces from the substrate to the cell interior due to the lower mechanical properties of the substrate, after ruling out the effect of fibronectin activity on the substrates that remain similar (in terms of the amount of adsorbed protein and distribution).

Experimental

Materials

Polymer sheets were obtained by radical polymerization of a solution of the corresponding alkyl acrylate, *i.e.* methyl (MA), ethyl (EA), butyl (BA), and hexyl (HA) (Sigma-Aldrich, Steinheim, Germany) using 0.2 wt% benzoin (98% pure, Scharlau, Barcelona, Spain) as a photoinitiator. The polymerization was carried out up to limiting conversion. After polymerization, low molecular-mass substances were extracted from the material by drying *in vacuo* to constant weight. Thin films were prepared by making use of a spin-coater (Brewer Science, Rolla, USA). To do that, each of the synthesized polymers was dissolved in toluene at a concentration of 2 wt%. Spin casting was performed on 12 mm glass coverslips at 2000 rpm for 30 s. Samples were dried *in vacuo* at 60 °C before further characterisation. The obtained films are not porous and are approximately 500 nm thick.

Water contact angles were measured using a Dataphysics OCA. The volume of the drop was 20 μl and the measurement was performed after 10 s of substrate-water contact.

Mechanical measurements were performed on a Perkin Elmer DMA device in the traction mode. The elastic modulus was recorded as a function of temperature; from −50 °C to 50 °C. Specimens were bars *ca.* 5 × 8 × 1 mm.

Atomic force microscopy, AFM

AFM experiments were performed using a Multimode AFM equipped with NanoScope IIIa controller from Veeco (Manchester, UK) operating in tapping mode in air. The Nanoscope 5.30r2 software version was used. Si-cantilevers from Veeco (Manchester, UK) were used with force constant of 2.8 N m^{-1} and resonance frequency of 75 kHz. The phase signal was set to zero at a frequency 5–10% lower than the resonance one. Drive amplitude was 600 mV and the amplitude setpoint A_{sp} was 1.8 V. The ratio between the amplitude setpoint and the free amplitude A_{sp}/A_0 was kept equal to 0.8.

Protein adsorption

Fibronectin from human plasma (Sigma, Barcelona, Spain) was adsorbed on the different substrates by immersing the material sheets in several FN solutions at concentrations of 2, 5, 20 and 50 μg ml^{-1} in PBS for 10 min. After adsorption, samples were rinsed in PBS to eliminate the non-adsorbed protein. The remaining drops on the surface were dried by exposing the sample to a nitrogen flow for 2-3 min. AFM was performed in the tapping mode immediately after sample preparation. Height, phase and amplitude magnitude were recorded simultaneously for each image.

To quantify the amount of adsorbed fibronectin, we measured the remaining protein in the supernatant, *i.e.* the amount of protein that remained in solution without adsorbing on the material surface, as explained elsewhere.[24] Different aliquots of non-adsorbed protein on substrates were subjected to 5% SDS polyacrylamide gel electrophoresis (PAGE), using Laemmli buffer 2x and denaturing standard conditions. Proteins were transferred to a positively charged polyvinylidene difluoride nylon membrane (GE Healthcare) using a semi-dry transfer cell system (Biorad), and blocked by immersion in 5% skimmed milk in PBS for 1 h at room temperature. The blot was incubated with anti-human fibronectin polyclonal antibody (developed in rabbit, Sigma) (1 : 500) in PBS and washed three times (10 min each) with PBS containing 0.1% Tween-20 and 2% skimmed milk. The blot was subsequently incubated in horseradish peroxidase-conjugated donkey anti-rabbit immunoglobulin G (GE Healthcare) diluted 1 : 20000 in PBS containing TWEEN 20 and 2% milk (1 h at room temperature). The enhanced chemiluminescence detection system (GE Healthcare) was used according to the manufacturer's instructions prior to exposing the blot to X-ray film for 1 min.

Image analysis of the western bands was done using in-house software developed under MATLAB R2009b (The MathWorks, Inc., Natick, MA, USA). All the western blotting bands were digitized using the same scanner (Epson Stylus Photo RX500, Seiko Epson Corpo., Nagano, Japan) and the same scan parameters: 8 bits gray scale image and 300 dpi. The digitized images were binarized using the Otsu method, which chooses the threshold that minimizes the intraclass variance of the thresholded black and white pixels, in order to create a mask that automatically selected the edge of each western blot band.[25] This mask was applied to a negative version of the original scanned picture providing a resulting image which contained only the western bands. The last step of the process consisted of adding all the pixels that conformed each band correctly weighted by their intensity level.

Cell culture

MC3T3-E1 cells were obtained from the RIKEN CELL BANK (Japan). Prior to seeding on FN-coated substrates, cells were maintained in DMEM medium supplemented with 10% foetal bovine serum and 1% penicillin-streptomycin and passaged twice a week using standard techniques.

Sample disks (12 mm diameter) placed in a 24-well tissue culture plate were coated with FN 20 μg ml^{-1} (2 h at 37 °C). Then, 10^4 cells were placed onto each substrate and were maintained at 37 °C in a humidified atmosphere under 5% CO_2 for 3 h. Each experiment was performed in triplicate.

Cell adhesion

After 3h of culture MC3T3-E1 cells were washed in Dulbecco's phosphate buffered saline (DPBS, Invitrogen) and fixed in 10% formalin solution (Sigma) at 4 °C for 1 h. Samples were then rinsed with DPBS and a permeabilizing buffer (103 g L^{-1} sucrose, 2.92 g L^{-1} NaCl, 0.6 g L^{-1} MgCl2, 4.76 g L^{-1} HEPES buffer, 5 mL L^{-1} Triton X-100, pH 7.2) was added at room temperature for 5 min. In order to reduce the background signal, samples were incubated in 1% BSA/DPBS at 37 °C for 5 min. Afterwards, samples were incubated in monoclonal mouse antibody against vinculin (1 : 400 in 1% BSA/DPBS; Sigma) at room temperature for 1 h. The samples were rinsed in 0.5% Tween 20/DPBS three times for 5 min each. Cy3-conjugated rabbit anti-mouse secondary antibody (1:200 in 1% BSA/DPBS; Jackson Immunoresearch) was then added at room temperature for 1h. Simultaneously, BODIPY FL phallacidin was added for the duration of this incubation (2–3 units/sample in 1% BSA/DPBS; Invitrogen). Finally, samples were washed before mounting in Vectashield containing DAPI (Vector Laboratories, Peterborough, UK). A Leica DM6000B fluorescent microscope was used for cellular imaging.

Fibronectin reorganization

The ability of cells to reorganise adsorbed FN (*i.e.*, early matrix) was monitored by coating all samples with 20 μg ml^{-1} at 37 °C, then rinsing with PBS twice, before seeding in a serum containing medium. The evolution of FN in the ECM was followed by immunofluorescence after 3h of culture. Afterwards, cells were washed in Dulbecco's phosphate buffered saline (DPBS, Invitrogen) and fixed in 10% formalin solution (Sigma) at 4 °C for 1 h. Samples were rinsed with DPBS and the permeabilization buffer was added at room temperature for 5 min. Samples were incubated with a polyclonal rabbit anti-FN antibody (1 : 400, Sigma), dissolved in 1% BSA/DPBS for 1 h, washed, and incubated with a goat anti-rabbit Cy3-conjugated secondary antibody (1:200 in 1% BSA/DPBS; Jackson Immunoresearch) for 1 h before washing and mounting with Vectashield containing DAPI.

Image analysis of focal contacts

The size distribution of the focal plaques was determined through a several-step image analysis including a contour delineation of the cell. For a perfect segmentation of the cell, (i) images showing the actin cytoskelton were grayscaled and equalized. (ii) The cell was then detected (segmented). Since the cytoskeleton differed greatly in contrast from the background image, a gradient-magnitude method (Sobel)[26–28] was applied to the image and once the gradient image was calculated, a binary mask was created containing the segmented cytoskeleton. (iii) Compared to the original image, the binary gradient mask showed gaps in the lines surrounding the cell (the outline of the object of interest was not completely delineated). These linear gaps disappeared when the Sobel image was dilated using linear structuring elements (a vertical structuring element followed by a horizontal one), obtaining a clear and perfect contour detection of the cell. Once the cell was perfectly segmented, the obtained binary mask was then applied to the image obtained in the red channel for vinculin. This permitted the focus of the attention on the cell and the focal adhesions, as any other object in the image

was virtually erased. This new image was then binarized through Otsu's method and size-filtered to avoid any extra small particles in the image that did not represent focal plaques of the size to be determined.[25] Once the sizes of the focal contacts were determined, a size distribution was easily obtained.

Conclusions

Subtle variations in substrate chemistry, namely the sequential addition of methyl groups in the side chain of a vinyl polymer, give rises to substrates with different mechanical stiffness and similar wettability. Even if the amount of adsorbed FN on each substrate remains constant, the distribution of the protein—its supramolecular assembly—on the substrate's surface is sensitive to minute changes in substrate chemistry: FN molecules remain globular and isolated on PMA but a well-interconnected FN network is formed on PEA, PBA and PHA. That is to say, one cannot compare the cellular behavior on PMA and the rest of the surfaces and ascribe their differences to the effect of substrate stiffness, as is usually done for other systems (*e.g.* increasing the crosslinking density in a gel) since there are qualitative differences in fibronectin activity among surfaces. This is a strong point in this work, the importance of accounting for the state of the protein layer at the cell-material interface before discussing cellular behavior in terms of the effects of substrate stiffness. Nevertheless, FN activity is similar on PEA, PBA and PHA, which allows one to focus on the effect of substrate stiffness on cell behavior, after confirming similar fibronectin adsorption and distribution on these substrates. Focal adhesions are larger on the stiffer substrates (PEA as compared to PBA and PHA), as well as the development of actin cytoskeleton, which points to higher transmission of forces between the cell and the adsorbed protein layer on stiffer substrates.

Acknowledgements

The support of the Spanish Ministry of Science and Innovation through project MAT2009-14440-C02-01 is kindly acknowledged. CIBER-BBN is an initiative funded by the VI National R&D&I Plan 2008-2011, Iniciativa Ingenio 2010, Consolider Program, CIBER Actions and financed by the Instituto de Salud Carlos III with assistance from the European Regional Development Fund. This work was supported by funds for research in the field of Regenerative Medicine through the collaboration agreement from the Conselleria de Sanidad (Generalitat Valenciana), and the Instituto de Salud Carlos III.

References

1 F. Grinnell, *J. Cell Biol.*, 1986, **103**, 2697.
2 U. S. Schwarz and I. B. Bischofs, *Med. Eng. Phys.*, 2005, **27**, 763.
3 J. Spie, *Ann. N. Y. Acad. Sci.*, 2002, **961**, 1.
4 C. Werner, T. Pompe and Salchert, *Adv. Polym. Sci.*, 2006, **203**, 63.
5 A. J. Garcia, *Adv. Polym. Sci.*, 2006, **203**, 171.
6 K. Anselme, M. Bigerelle, B. Noel, E. Dufresne, D. Judas, A. Iost and P. Hardouin, *J. Biomed. Mater. Res.*, 2000, **49**, 155.
7 R. O. Hynes, *Cell*, 2002, **110**, 673.
8 B. Geiger, A. Bershadsky, R. Pankov and K. M. Yamada, *Nat. Rev. Mol. Cell Biol.*, 2001, **2**, 793.
9 J. M. Anderson, *Annu. Rev. Mater. Res.*, 2001, **31**, 81.
10 J. Y. Wong, J. B. Leach and X. Q. Brown, *Surf. Sci.*, 2004, **570**, 119.
11 D. S. Gray, J. Tien and C. S. Chen, *J. Biomed. Mater. Res.*, 2003, **66a**, 605.
12 N. G. Genes, J. A. Rowley, D. J. Mooney and L. J. Bonassar, *Arch. Biochem. Biophys.*, 2004, **422**, 161.
13 A. Schneider, G. Francius, R. Obeid, P. Schwinté, J. Hemmerlé, B. Frisch, P. Schaaf, J. C. Voegel, B. Senger and C. Picart, *Langmuir*, 2006, **22**, 1193.
14 P. L. Ryan, R. A. Foty, J. Kohn and M. S. Steinberg, *Proc. Natl. Acad. Sci. U. S. A.*, 2001, **98**, 4323.
15 J. Y. Wong, A. Velasco, P. Rajagopalan and Q. Pham, *Langmuir*, 2003, **19**, 1908.
16 C. M. Lo, H. B. Wang, M. Dembo and Y. L. Wang, *Biophys. J.*, 2000, **79**, 144.
17 I. B. Bischofs and U. S. Schwarz, *Proc. Natl. Acad. Sci. U. S. A.*, 2003, **100**, 9274.
18 U. S. Schwarz, *Soft Matter*, 2007, **3**, 263.
19 D. Choquet, D. P. Fenselfeld and M. P. Sheetz, *Cell*, 1997, **88**, 39.
20 V. Vogel and M. P. Sheetz, *Nat. Rev. Mol. Cell Biol.*, 2006, **7**, 265.
21 D. E. Discher, P. Janmey and Y. Wang, *Science*, 2005, **310**, 1139.
22 D. Harjanto and M. H. Zaman, *Org. Biomol. Chem.*, 2010, **8**, 299.
23 R. J. Pelham and Y. L. Wang, *Proc. Natl. Acad. Sci. U. S. A.*, 1997, **94**, 13661.
24 P. Rico, J. C. Rodríguez Hernández, D. Moratal, M. Monleón Pradas, G. Altankov and M. Salmerón-Sánchez, *Tissue Eng. A*, 2009, **15**, 3271.
25 N. A. Otsu, *IEEE Trans. Syst. Man Cybern.*, 1979, **9**, 62.
26 R. C. Gonzalez, R. E. Woods and S. L. Eddins, *Digital Image Processing using MATLAB*, Prentice-Hall, NJ, U.S.A, 2003.
27 R. C. Gonzalez, R. E. Woods, *Digital Image Processing*, Prentice-Hall, Upper Saddle River, NJ, U.S.A, 2007.
28 *MATLAB Image Processing Toolbox User's Guide*, The MathWorks, Inc., Natick, MA, U.S.A, 2006.
29 G. Altankov, V. Thom, T. Groth, K. Jankova, G. Jonsson and M. Ulbricht, *J. Biomed. Mater. Res.*, 2000, **52**, 219.
30 A. J. García and D. B. Boettiger, *Biomaterials*, 1999, **20**, 2427.
31 A. J. Engler, S. Sen, H. L. Sweeney and D. E. Discher, *Cell*, 2006, **126**, 677.
32 B. G. Keselowsky, C. M. Collard and A. J. Garcia, *Proc. Natl. Acad. Sci. U. S. A.*, 2005, **102**, 5953.
33 C. C. Barrias, M. C. L. Martins, G. Almeida-Porada and M. A. Barbosa, *Biomaterials*, 2009, **30**, 307.
34 C. B. Khatiwala, S. R. Peyton and A. J. Putnam, *Am. J. Physiol.: Cell Physiol.*, 2006, **290**, C1640.
35 H. J. Kong, T. H. Polte, E. Alsberg and D. J. Mooney, *Proc. Natl. Acad. Sci. U. S. A.*, 2005, **102**, 4300.
36 B. G. Keselowsky, D. M. Collard and A. J. García, *Biomaterials*, 2004, **25**, 5947.
37 B. G. Keselowsky, D. M. Collard and A. J. García, *J. Biomed. Mater. Res.*, 2003, **66a**, 247.
38 D. Gugutkov, C. González-García, J. C. Rodríguez Hernández, G. Altankov and M. Salmerón-Sánchez, *Langmuir*, 2009, **25**, 10893.
39 D. Gugutkov, G. Altankov, J. C. Rodríguez Hernández, M. Monleón Pradas and M. Salmerón Sánchez, *J. Biomed. Mater. Res., Part A*, 2010, **92a**, 322.
40 Y. H. Bae, P. A. Johnson, C. A. Florek, J. Kohn and P. V. Moghe, *Acta Biomater.*, 2006, **2**, 473.
41 A. Nicolas, B. Geiger and S. A. Safran, *Proc. Natl. Acad. Sci. U. S. A.*, 2004, **101**, 12520.
42 N. Q. Balaban, U. S. Schwarz, D. Riveline, P. Goichberg, G. Tzur, I. Sabanay, D. Mahalu, S. A. Safran, A. S. Bershadsky, L. Addali and B. Geiger, *Nat. Cell Biol.*, 2001, **3**, 466.